

Relationship between Two-Photon Absorption and the π -Conjugation Pathway in Porphyrin Arrays through Dihedral Angle Control

Tae Kyu Ahn,[†] Kil Suk Kim,[†] Deok Yun Kim,[†] Su Bum Noh,[†] Naoki Aratani,[‡] Chusaku Ikeda,[‡] Atsuhiko Osuka,^{*,‡} and Dongho Kim^{*,†}

Contribution from the Center for Ultrafast Optical Characteristics Control and Department of Chemistry, Yonsei University, Seoul 120-749, Korea, and Department of Chemistry, Graduate School of Science, CREST of JST, Kyoto University, Kyoto 606-8502, Japan

Received October 12, 2005; E-mail: dongho@yonsei.ac.kr; osuka@kuchem.kyoto-u.ac.jp

Abstract: Recently, covalently linked or self-assembled porphyrin array systems have attracted much attention for their enhanced two-photon absorption (TPA) behaviors. In this study, we have investigated the TPA properties of various dihedral angle controlled, directly linked porphyrin dimers and arrays to elucidate the relationship between the π -conjugation pathway and TPA properties. We have demonstrated a strong correlation between π -conjugation (aromaticity) and TPA properties in porphyrin assemblies.

Introduction

Recently, π -conjugated organic molecules have attracted much attention as soft processable optical nonlinear materials in light of their intensity-dependent refractive index and nonlinear absorption properties, because these features can find versatile applications in two-photon laser scanning fluorescence microscopy, optical power limiting, three-dimensional optical storage, micro-fabrication and up-converted lasing.¹ In this context, porphyrins are promising candidates for third-order nonlinear optical (NLO) properties, such as two-photon absorption (TPA).² While porphyrin monomers that possess 18 π -electrons to exhibit aromaticity have only a small TPA cross-section (<100 GM), peripheral conjugated substituents or formation of intermolecular porphyrin assemblies enhances significantly the TPA cross-section values.³ Representative molecular designs utilize a donor(D)/acceptor(A) separated by the π -conjugation system to increase the charge separation efficiency (D- π -D, A- π -A, D- π -A),⁴ to covalently link porphyrin oligomers with triple bond linkages, hence leading to coplanar geometry between the neighboring porphyrin moieties and, as a consequence, ensuring resonance structures with large charge

separation,⁵ and to form porphyrin assemblies.^{6–8} Large TPA cross-sections thus achieved have often been ascribed to effective π -delocalization that leads to a large conjugated network, but the molecular mechanism has been only poorly understood.

In this paper, we have examined the TPA properties of directly *meso-meso*-linked porphyrin arrays with a particular attention to their dependence upon the dihedral angle between the neighboring porphyrins. Systematic control of the dihedral angle of the directly linked *meso-meso* diporphyrins can offer a fine-tuning of electronic interactions between the two porphyrin units.⁹ We believe that this feature influences significantly the π -conjugation effect over the two porphyrin moieties and eventually the TPA properties mainly determined by charge separation behaviors. We have attempted to control the degree of π -conjugation in porphyrin arrays by changing the dihedral angles between the neighboring porphyrin units via the variation of strapped chain length, axial ligand coordination, host–guest interactions through hydrogen bonding, and complete flat structures in porphyrin arrays (Chart 1). The objective of the present study is to provide a firm basis for understanding of TPA properties of *meso-meso*-linked porphyrin arrays, which will be useful for further investigations of TPA properties in other types of molecular assemblies.

Results and Discussion

Dihedral Angle Control via Covalent Strap Chain. The directly linked *meso-meso* diporphyrins (Chart 1, **Z2**) are

- (5) Zhang, T.-G.; Zhao, Y.; Asselberghs, I.; Persoons, A.; Clays, K.; Therien, M. J. *J. Am. Chem. Soc.* **2005**, *127*, 9710–9720.
- (6) Ogawa, K.; Zhang, T.; Yoshihara, K.; Kobuke, Y. *J. Am. Chem. Soc.* **2002**, *124*, 22–23.
- (7) Ogawa, K.; Ohashi, A.; Kobuke, Y.; Kamada, K.; Ohta, K. *J. Am. Chem. Soc.* **2003**, *125*, 13356–13357.
- (8) Drobizhev, M.; Stepanenko, Y.; Dzenis, Y.; Karotki, A.; Rebane, A.; Taylor, P. N.; Anderson, H. L. *J. Am. Chem. Soc.* **2004**, *126*, 15352–15353.
- (9) Aratani, N.; Osuka, A.; Kim, Y. H.; Jeong, D. H.; Kim, D. *Angew. Chem., Int. Ed.* **2000**, *112*, 1517–1521.

[†] Yonsei University.

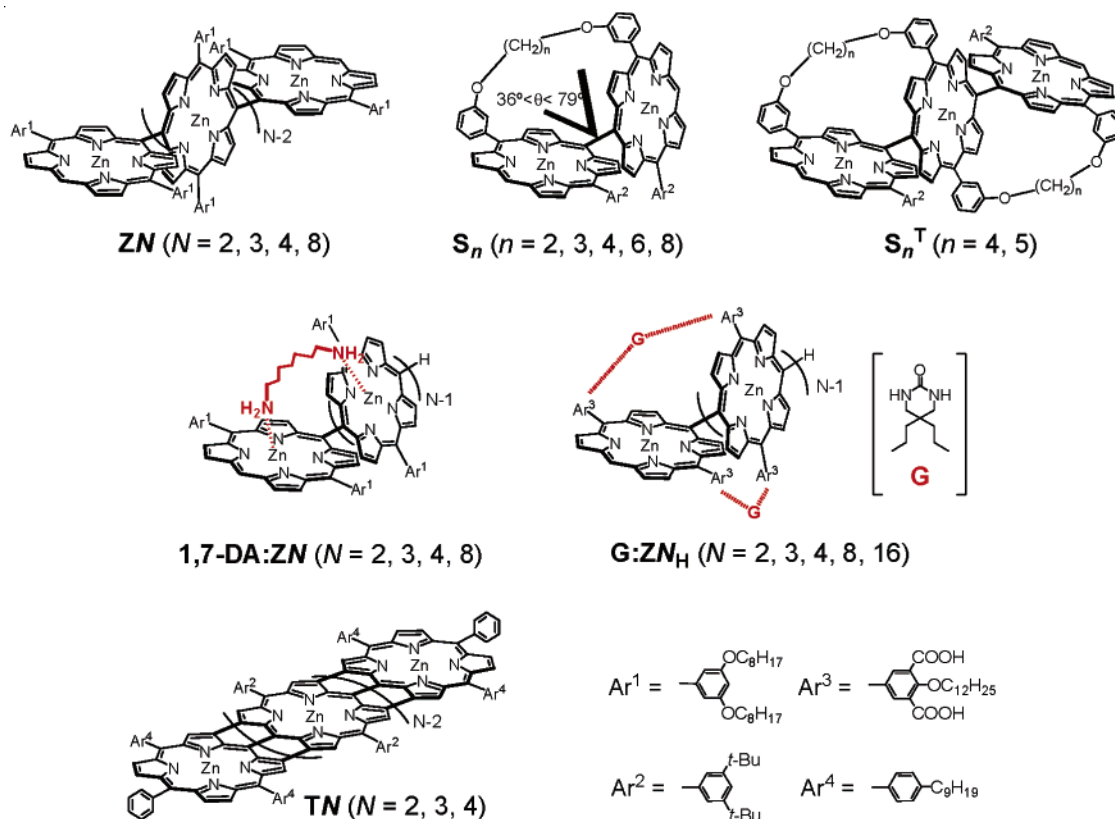
[‡] Kyoto University.

- (1) Lin, T.-C.; Chung, S.-J.; Kim, K.-S.; Wang, X.; He, G. S.; Swiatkiewicz, J.; Pudavar, H. E.; Prasad, P. N. *Adv. Polym. Sci.* **2003**, *161*, 157–193.
- (2) If we identify the *i*-state with the intermediate state, and the two-photon allowed state is assigned to the final state, *f*, the second-order perturbation theory expresses the TPA cross-section values as follows.

$$\sigma_2^{\max} = \frac{(2\pi)^4 (2\cos^2\theta + 1)}{15} \sqrt{\frac{\ln 2}{\pi}} \frac{L^4}{(\hbar c n)^2} \frac{|\mu_{i0}|^2 |\mu_{fi}|^2}{\Gamma_f} \left(\frac{\nu_{i0}}{\nu_{f0}} - \frac{1}{2} \right)^{-2}$$

where n is the refractive index of medium, $L = (n^2 + 2)/3$ is the local field factor, A_f is the line width of the *f*-th state, and θ is the angle between the two transition dipole moment vectors, μ_{i0} and μ_{fi} .

- (3) Kadishi, K. M.; Smith, K. M.; Guillard, R. *The Porphyrin Handbook*; Academic Press: Oxford, UK, 2003; Vols. 1–20.
- (4) Albota, M. et al. *Science* **1998**, *281*, 1653–1650.

Chart 1. Molecular Structures of **ZN**, **S_n**, **S_n^T**, **1,7-DA:ZN**, **G:ZN_H**, and **TN**

considered to maintain the average dihedral angle of 90° due to a large steric hindrance between the adjacent porphyrin planes, leading to minimum electronic interactions (Supporting Information (SI), Figure S1 and Table S1).⁹ This feature also gives rise to very small TPA values of <100 GM in **ZN** ($N = 2, 3, 4, \dots$), which is nearly comparable to that of the porphyrin monomer. Therefore, tilting of a porphyrin ring toward the other porphyrin plane would increase the electronic interactions through enhancement of π -conjugation along the two porphyrin units and simultaneously enhance the TPA properties. We thus examined the TPA properties of a series of strapped *meso-meso*-linked diporphyrins in which the dihedral angle of the diporphyrins is systematically changed by introducing a dioxymethylene strap varying the number of carbon atoms (**S_n**, $n = 6, 5, 4, 3, 2$, and 1) between the two porphyrins.¹⁰ The dihedral angles have been calculated as follows: 80° (**S₆**), 77° (**S₅**), 71° (**S₄**), 48° (**S₃**), 42° (**S₂**), and 36° (**S₁**). As the dihedral angle is reduced, the absorption spectra of **S_n** exhibit more prominently split Soret bands as well as enhanced charge transfer (CT) bands, reflecting increased electronic interactions between the two porphyrin planes (SI, Figure S2).¹⁰ The calculated absorption spectra of strapped diporphyrins with a reduced dihedral angle by the INDO/S-SCI method, which matches well with their corresponding absorption spectra, exhibit more intense CT absorption bands with the decrease in the dihedral angle (SI, Figures S3 and S4). On the other hand, the fluorescence quantum yields and their lifetimes are not so significantly perturbed with the decrease in the strap chain length compared with those of **Z2** (Table 1).

Table 1. TPA Cross-Section $\sigma^{(2)}$ (GM) Values, Fluorescence Quantum Yields, and Excited Singlet-State Lifetimes of **S_n**, **S_n^T**, **1,7-DA:ZN**, **G:ZN_H**, and **TN** in Toluene

sample	$\sigma^{(2)}$ (GM) ^f	Φ_F	τ_{S1}
S1^a	7500	0.023	1.37 ns
S2	6330	0.028	1.49 ns
S3	6120	0.028	1.61 ns
S4	4830	0.027	1.70 ns
S5	3920	0.030	1.73 ns
S6	3470	0.030	1.78 ns
S4^T	6550	0.046	1.64 ns
S5^T	4650	0.041	1.67 ns
1,7-DA:Z2^{b,c}	4810	0.038	1.74 ns
1,7-DA:Z3	2930	0.038	1.65 ns
1,7-DA:Z4	<100	0.046	1.57 ns
1,7-DA:Z8	<100	0.063	1.49 ns
G:Z2^d	4500	0.045	1.87 ns
G:Z3_H	9500	0.063	1.62 ns
G:Z4_H	11800	0.087	1.60 ns
G:Z8_H	12800	0.111	1.47 ns
G:Z16_H	13200	0.187	1.20 ns
T2^e	11900 ^g	<i>h</i>	4.5 ps
T3	33100		2.9 ps
T4	93600		0.72 ps

^a Concentration: 0.25 mM in toluene. ^b Concentration: 0.42 mM in toluene. ^c 5% of **1,7-DA** is added to the **ZN** solution. ^d Concentration: 0.12 mM in toluene. ^e Concentration: 0.1 mM in toluene with 5% *n*-butylamine. ^f Excitation at 800 nm. ^g Excitation at 1200 nm. ^h Nonfluorescent.

The TPA cross-section values of a series of strapped diporphyrins **S_n** were measured in toluene by using an open-aperture Z-scan method with excitation at 800 nm, where no ground-state absorption was observed (Table 1). Even a slight reduction in the dihedral angle for **S₆** leads to a large enhancement in TPA cross-section values as compared with a negligible TPA value for orthogonal diporphyrin **Z2**, indicating that the electronic interactions between the two porphyrin planes are

(10) Yoshida, N.; Ishizuka, T.; Osuka, A.; Jeong, D. H.; Cho, H. S.; Kim, D.; Matsuzaki, Y.; Nogami, A.; Tanaka, K. *Chem.—Eur. J.* **2003**, *9*, 58–75.

sensitive to the dihedral angle. Thus, the intense CT bands induced by strong electronic interactions between the adjacent porphyrin monomers indicate the effective charge separation, leading to large TPA cross-section values. As shown in Table 1, we notice clearly that the TPA values increase systematically in a series of strapped diporphyrins S_n as the dihedral angle is reduced upon the decrease in the strap chain length (SI, Figure S5). This feature illustrates that there is a strong correlation between the NLO properties such as TPA cross-section values and the π -conjugation pathway of porphyrin dimers. We have extended our TPA measurements to strapped triporphyrins S_4^T and S_5^T (Chart 1 and SI, Figure S6), which are the extensions of S_4 and S_5 diporphyrins, to investigate the effect of increased π -conjugation over the three porphyrin moieties on the TPA properties (Table 1). We have observed the enhancement of TPA values as compared with the corresponding dimers, indicating that the elongation of the π -conjugation pathway throughout the porphyrin array would lead to the increased NLO properties.

Dihedral Angle Control via Coordination. We have attempted to control the dihedral angle of diporphyrins through the coordination of 1,7-diaminoheptane (**1,7-DA**) simultaneously onto the two Zn(II) metals in the diporphyrin **Z2** (Chart 1) since **1,7-DA** has been shown to be the most effective for reducing the dihedral angle.¹¹ On the basis of the changes in the absorption and fluorescence spectra of *meso-meso*-linked diporphyrins upon the addition of **1,7-DA**, we can demonstrate that the association of **1,7-DA** with **Z2** occurs through two amino groups coordinated simultaneously to the two Zn(II) centers, consequently forcing a tilt of the dihedral angle between the two porphyrin planes, resembling the absorption spectra of strapped diporphyrin **S4** (SI, Figure S7).¹¹ It is interesting to note that the TPA cross-section value measured for the **1,7-DA:Z2** adduct at 800 nm is comparable to that of **S4** (Table 1 and SI, Figure S8). We have explored the TPA values for **1,7-DA:Z3**, **1,7-DA:Z4**, and **1,7-DA:Z8** adducts with an expectation of enhanced TPA values through the elongated π -conjugation pathway.

For the **1,7-DA:Z3** adduct, however, the decreased TPA value was obtained as compared with that of **1,7-DA:Z2**, indicating that the π -conjugation pathway is only limited to the diporphyrin unit, and as a consequence, the nearly orthogonal geometry between **1,7-DA:Z2** and the remaining porphyrin monomer (probably coordinated to one amine unit of **1,7-DA**) in **1,7-DA:Z3** prohibits the π -conjugation pathway from extending into the whole **Z3** trimer. Thus, the arguments that the prohibition of π -conjugation by the orthogonality between non- or mono-coordinated adjacent Zn(II) porphyrin moieties plays a major role in reducing the TPA values can also be supported by the observation of negligible TPA values in **1,7-DA:Z4** and **1,7-DA:Z8** adducts (Table 1).¹² Thus, even in porphyrin arrays, the control of the dihedral angle in a consecutive manner is crucial for attaining large TPA values through the π -conjugation pathway over the whole array system without interruption of π -conjugation.

Dihedral Angle Control via Host/Guest Interactions. We have tried to control the dihedral angle between the adjacent porphyrin planes in the *meso-meso*-linked Zn(II) porphyrin arrays (**ZN**) by inserting *meso*-aryl substituents with hydrogen bonding between carboxyl groups and a cyclic urea guest (**G**) (Chart 1). *Meso-meso*-linked porphyrin oligomers, **ZN_H** ($N = 2, 3, 4, 8,$ and 16), were prepared via Ag(I)-promoted coupling of the porphyrin monomer **Z1_{Me}** followed by hydrolysis of ester groups.¹³ As the guest molecule **G** was added to **ZN_H** solution, the absorption spectral changes are consistent with the dihedral angle reduction observed in strapped diporphyrins S_n (SI, Figures S9–S11).

We have measured the TPA cross-section values for a series of **G:ZN_H** ($N = 2, 3, 4, 8,$ and 16) arrays at 800 nm. The TPA cross-section values increase and start to show a saturation behavior at **G:Z4_H** as the array becomes longer (Table 1 and SI, Figure S12). Especially, the TPA value for **G:Z3_H** is much larger than that of **1,7-DA:Z3**, illustrating that a continuous dihedral angle reduction in a helical way throughout the whole **Z3** trimer via hydrogen bonding in **G:Z3_H** enhances the π -conjugation pathway along the trimer, and thus much enhanced TPA properties were observed. It is noteworthy that a further enhancement in the TPA cross-section values was not observed in longer arrays, such as **G:Z8_H** and **G:Z16_H**, with a saturation of the TPA value of $\sim 12\,000$ GM at **G:Z4_H**. This feature can be explained by the fact that a consecutive dihedral angle reduction via clipping with guest urea molecules in the *meso-meso*-linked array leads to one complete turn of the porphyrin plane in **G:Z4_H**, with the two end porphyrin planes nearly coplanar (SI, Figures S10 and S11). Thus, even in longer arrays than the tetramer, further enhancement of the π -conjugation pathway throughout the whole array does not take place, which also explains a saturation behavior in the TPA values for a series of **G:ZN_H** ($N = 2, 3, 4, 8,$ and 16) arrays. However, maintenance of relatively large TPA values in longer arrays than **G:Z4_H** is presumably due to a continuous reduction of the dihedral angle between the adjacent porphyrin planes throughout the array, which ensures a helical linear structure of the array (Table 1 and SI, Figure S12). This feature is in a sharp contrast with the negligible TPA values observed in **1,7-DA:Z4** and **1,7-DA:Z8** arrays. It is noteworthy that the fluorescence quantum yields of a series of **G:ZN_H** ($N = 2, 3, 4,$ and 8) are significantly enhanced as compared with those of their corresponding **ZN** arrays.

Complete Coplanar Structures. The way to achieve full π -conjugation between the adjacent porphyrins is to make multiple covalent linkages between porphyrins. For this goal, the synthesis of *meso-meso*, β - β , and β - β triply linked Zn(II) porphyrin tapes (**TN**, $N = 2, 3,$ and 4) from corresponding

(11) Shimori, H.; Ahn, T. K.; Cho, H. S.; Kim, D.; Yoshida, N.; Osuka, A. *Angew. Chem., Int. Ed.* **2003**, *115*, 2860–2864.

(12) It is possible that three or more consecutive Zn(II) porphyrins are each ligated with one **1,7-DA**, although the probability is low. As Zn(II) porphyrins in the **ZN** array are each ligated with one **1,7-DA**, the bathochromic shift in absorption spectra should be small (~ 5 nm), as illustrated by the coordination with pyridine. Thus, much larger red-shifted absorption, as shown in the absorption spectra of **1,7-DA:ZN** (SI, Figure S7), indicate that there are simultaneously coordinated Zn(II) porphyrin dimer units by **1,7-DA** in **ZN** porphyrin arrays. Thus, the combination of the dilution effect by non- or mono-coordinated Zn(II) porphyrins and the orthogonality between the two bis-coordinated Zn(II) porphyrin dimer units would reduce the TPA values. In any cases, the prohibition of π -conjugation by the orthogonality between Zn(II) porphyrin moieties plays a major role in reducing the TPA values.

(13) Ikeda, C.; Yoon, Z. S.; Park, M.; Inoue, H.; Kim, D.; Osuka, A. *J. Am. Chem. Soc.* **2005**, *127*, 534–535.

orthogonal porphyrin arrays **ZN** is ideally suited (Chart 1).¹⁴ The porphyrin tapes **TN** thus prepared exhibit a continuous red-shift of the lowest Q-band transitions that penetrate into the infrared region, indicating that **TN** arrays are fully conjugated over the whole array (SI, Figure S13).¹⁵ The X-ray structure of **T2** shows that the two porphyrin rings are fused to form a coplanar saddle-like conformation with a mean plane deviation of 0.16 Å. However, **TN** arrays exhibit aggregation phenomena due to their self-assembling nature by π - π stacking. Thus, we have employed *n*-butylamine to dissociate **TN** aggregates in solution, which is confirmed by the absorption spectral changes. In addition, the calculated absorption spectra by the PPP-SCI method show intense CT bands which allude to large TPA cross-section values due to charge separation (SI, Figure S14).¹⁵

We have measured the TPA cross-section values of **TN** in solution at 1200 nm, where the ground-state absorption is minimal. As seen in Table 1, a continuous increase in the TPA values of **TN** was observed as the array becomes longer, illustrating the elongation of the π -conjugation pathway throughout the whole array (SI, Figure S15).¹⁶ Since the absorption of **TN** occurs in all spectral ranges down to the IR region, it becomes difficult to choose the excitation wavelength suitable for negligible ground-state contributions to the TPA values. Even considering the weak ground-state contribution of **TN** at 1200 nm, the TPA values of **TN**, especially **T4**, are the largest ones, to the best of our knowledge, ever reported in single chromophore macrocyclic dyes.

We have also investigated the excited-state dynamics by femtosecond transient absorption measurements to explore the relationship between the TPA processes and the excited-state dynamics of **TN**. We observed ~ 4.5 ps lifetime for the S_1 state of **T2**, which is much faster than that of the Zn(II) porphyrin monomer (~ 2.6 ns) and its orthogonal dimer **Z2** (~ 1.8 ns) (SI, Figure S16). Moreover, the S_1 state lifetimes of **TN** become shorter, indicating that a much reduced HOMO-LUMO gap of **TN** accelerates the S_1 state decay via nonradiative decay channels (Table 1). The contribution to the TPA values at 1200 nm by the excited-state absorption seems to be not so significant as revealed by the relatively weak and featureless transient absorption of **TN** at 1200 nm. Thus, the transient absorption spectral features as well as the relatively short excited-state lifetimes of **TN** suggest that the TPA processes in **TN** are contributed to by simultaneous two-photon absorption via S_1 manifolds as intermediate states.¹⁷ The large TPA cross-section values of **TN** observed in our investigations suggest that π -electron delocalization through the porphyrin array framework and the completely flat structures are the determining factors to enhance the NLO properties.

Conclusion

We have controlled systematically the dihedral angles of directly linked porphyrin dimers and arrays to explore the

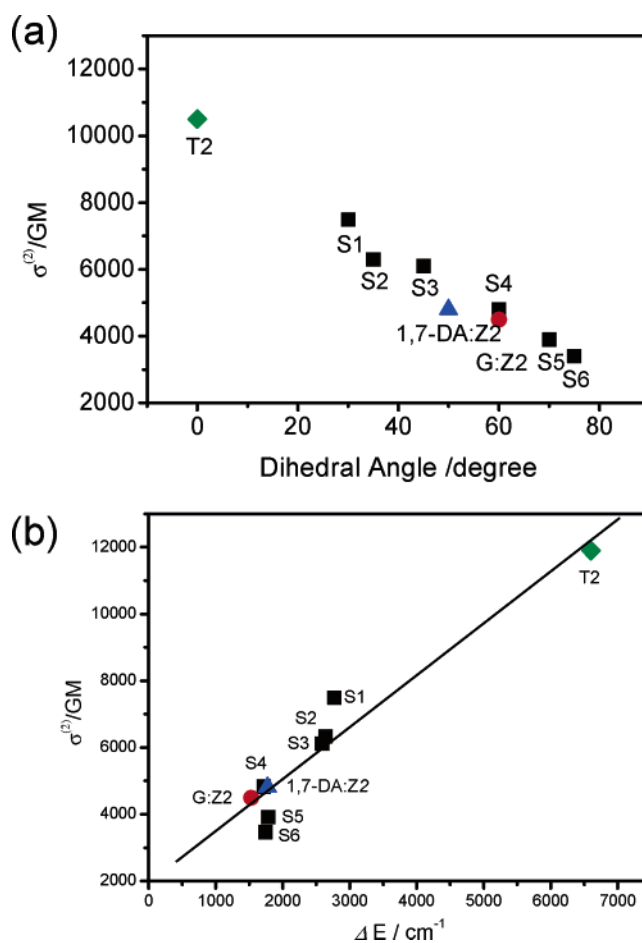


Figure 1. (a) The plot of TPA cross-section ($\sigma^{(2)}$) values of various Zn(II) porphyrin dimers versus dihedral angle. (b) The plot of TPA cross-section ($\sigma^{(2)}$) values of various Zn(II) porphyrin dimers versus splitting energy in B-band absorption.

relationship between the π -conjugation effect of the adjacent porphyrin planes and the TPA values. Our study demonstrates that the enhancement in electronic interactions in various porphyrin arrays upon reduction of the dihedral angle is strongly correlated with the large TPA cross-section values (Figure 1). The complete flat molecular geometries in porphyrin tapes **TN** lead to much larger TPA cross-section values induced by nearly complete π -electron delocalization without interruption throughout the whole array skeleton. We believe that our investigations provide a guideline for further search of new types of organic NLO materials. Finally, the fused porphyrin arrays **TN** have proved to be a promising candidate for future applications in NLO devices.

Experimental Section

Fluorescence Lifetime Measurements. Time-resolved fluorescence was detected using a time-correlated single-photon-counting (TCSPC) technique. As an excitation light source, we used a home-made cavity dumped Ti:sapphire oscillator, which provided a high repetition rate (200–400 kHz) of ultrashort pulses (100 fs at full width half-maximum (fwhm)) pumped by a CW Nd:YVO₄ laser (Spectra-Physics, Millennia). The output pulses of the oscillator were frequency-doubled with a second harmonic crystal. The TCSPC detection system consisted of a microchannel plate photomultiplier (Hamamatsu, R3809U-51) with a cooler (Hamamatsu, C4878), a TAC (EG&G Ortec, 457), two discriminators (EG&G Ortec, 584 (signal) and Canberra, 2126 (trigger)), and two wideband amplifiers (Philip Scientific (signal) and Mini Circuit

(14) Tsuda, A.; Osuka, A. *Science* **2001**, *293*, 79–82.

(15) Cho, H. S.; Jeong, D. H.; Cho, S.; Kim, D.; Matsuzaki, Y.; Tanaka, K.; Tsuda, A.; Osuka, A. *J. Am. Chem. Soc.* **2002**, *124*, 14642–14654.

(16) While the lowest absorption transitions in **TN** are continuously red-shifted, the TPA values reach the maximum at **T4** and decrease in **T6** and **T8** as the array becomes longer. Although *n*-butylamine was added to **T6** and **T8** solutions to prevent aggregation phenomena, there still exists a possibility of aggregation formation, especially in **T6** and **T8**, leading to reduced TPA values.

(17) Kim, D. Y.; Ahn, T. K.; Kwon, J. H.; Kim, D.; Ikeue, T.; Aratani, N.; Osuka, A.; Shigeiwa, M.; Maeda, S. *J. Phys. Chem. A* **2005**, *109*, 2996–2999.

(trigger). A personal computer with a multichannel analyzer (Canberra, PCA3) was used for data storage and processing. The overall instrumental response function was about 60 ps (fwhm).

Femtosecond Transient Absorption Measurements. The dual-beam femtosecond time-resolved transient absorption spectrometer consisted of a self-mode-locked femtosecond Ti:sapphire laser (Coherent, MIRA), a Ti:sapphire regenerative amplifier (Clark MXR, CPA-1000) pumped by a Q-switched Nd:YAG laser (ORC-1000), a pulse stretcher/compressor, OPG-OPA system, and an optical detection system.¹⁸ The pump beam was focused to a 1 mm diameter spot, and laser fluence was adjusted to less than $\sim 1.0 \text{ mJ cm}^{-2}$ by using a variable neutral-density filter. The fundamental beam remaining in the OPG-OPA system was focused onto a flowing water cell to generate a white light continuum, which was again split into two parts. The one part of the white light continuum was overlapped with the pump beam at the sample to probe the transient, while the other part of the beam was passed through the sample without overlapping the pump beam. The time delay between pump and probe beams was controlled by making the pump beam travel along a variable optical delay. The white continuum beams after sampling were sent to a 15 cm focal length spectrograph (Acton Research) through each optical fiber and then detected by the dual 512 channel photodiode arrays (Princeton Instruments). The intensity of the white light of each 512 channel photodiode array was processed to calculate the absorption difference spectrum at the desired time delay between pump and probe pulses.

Measurement of the Two-Photon Absorption Cross-Section ($\sigma^{(2)}$). The TPA spectra were measured at 800 and 1200 nm by using the open-aperture Z-scan method¹⁹ with ~ 130 fs pulses from an optical parametric amplifier (Light Conversion, TOPAS) operating at a 5 kHz repetition rate generated from a Ti:sapphire regenerative amplifier system (Spectra-Physics, Hurricane) (SI, Figure S17). The laser beam was divided into two parts. One was monitored by a Ge/PN photodiode (New Focus) as the intensity reference, and the other was used for transmittance measurement. After passing through an $f = 10$ cm lens, the laser beam was focused and passed through a quartz cell. The position of the sample cell could be varied along the laser-beam direction (z -axis), so the local power density within the sample cell

could be changed under a constant laser power level. The thickness of the cell was 1 mm. The transmitted laser beam from the sample cell was then detected by the same photodiode as used for reference monitoring. The on-axis peak intensity of the incident pulses at the focal point, I_0 , ranged from 40 to 60 GW cm^{-2} . Assuming a Gaussian beam profile, the nonlinear absorption coefficient β can be obtained by curve fitting to the observed open-aperture traces with the following equation:

$$T(z) = 1 - \frac{\beta I_0 (1 - e^{-\alpha_0 l})}{2\alpha_0 (1 + (z/z_0)^2)} \quad (1)$$

where α_0 is the linear absorption coefficient, l the sample length, and z_0 the diffraction length of the incident beam.

After obtaining the nonlinear absorption coefficient β , the TPA cross-section $\sigma^{(2)}$ of one solute molecule (in units of $1 \text{ GM} = \text{cm}^4 \cdot \text{s}/\text{photon} \cdot \text{molecule}$) can be determined by using the following relationship:

$$\beta = \frac{\sigma^{(2)} N_A d \times 10^{-3}}{h\nu} \quad (2)$$

where N_A is the Avogadro constant, d is the concentration of the TPA compound in solution, h is the Planck constant, and ν is the frequency of the incident laser beam.

We obtained the TPA cross-section $\sigma^{(2)}$ values at the corresponding wavelength, where linear absorption is negligible, to satisfy the condition of $\alpha_0 l \ll 1$ in retrieving the pure TPA $\sigma^{(2)}$ values in the simulation procedure. We also measured the TPA cross-section value of AF-50 as a reference compound, which exhibits 50 GM at 800 nm.

Acknowledgment. This work was financially supported by the National Creative Research Initiatives Program of the Korea Science Engineering Foundation (D.K.) and the CREST program of JSP (A.O.).

Supporting Information Available: Synthesis, complete ref 4, Z-scan setup, absorption spectra, calculated MOs, calculated absorptions, X-ray crystal structure, transient absorption decay profiles, and Z-scan curves of samples are available. This material is available free of charge via the Internet at <http://pubs.acs.org>.

JA056773A

(18) Cho, H. S.; Song, N. W.; Kim, Y. H.; Jeoung, S. C.; Hahn, S.; Kim, D.; Kim, S. K.; Yoshida, N.; Osuka, A. *J. Phys. Chem. A* **2000**, *104*, 3287–3298.

(19) Sheik-Bahae, M.; Said, A. A.; Wei, T.-H.; Hagan, D. G.; van Stryland, E. W. *IEEE J. Quantum Electron.* **1990**, *26*, 760–769.